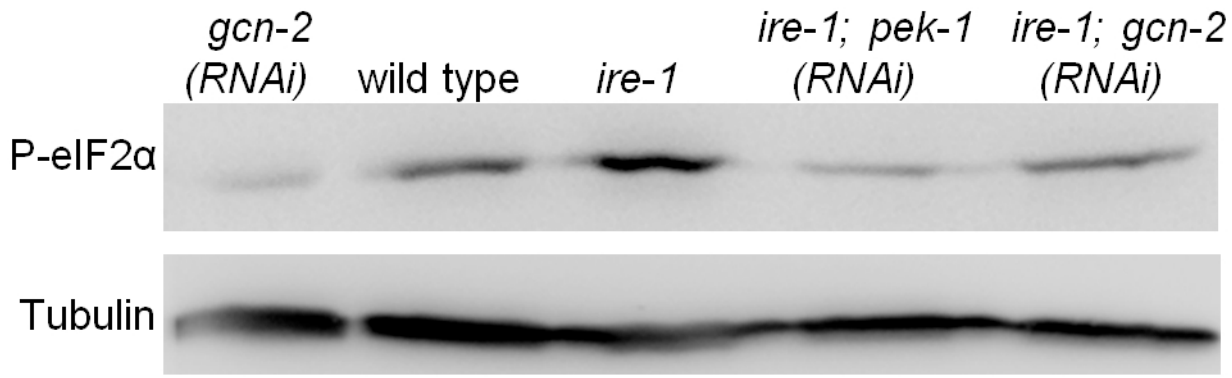

Fig. S1. Phosphorylation of eIF2α by PEK-1 is increased in *ire-1* mutants. Representative western blot of phosphorylated eIF2α and tubulin of day-0 wild-type animals and *ire-1* mutants treated with control, *pek-1* or *gcn-2* RNAi. Note that whereas in wild-type animals eIF2α phosphorylation was mostly *gcn-2* dependent, in *ire-1* mutants eIF2α phosphorylation was mostly *pek-1* dependent. This experiment was repeated three times with similar results.

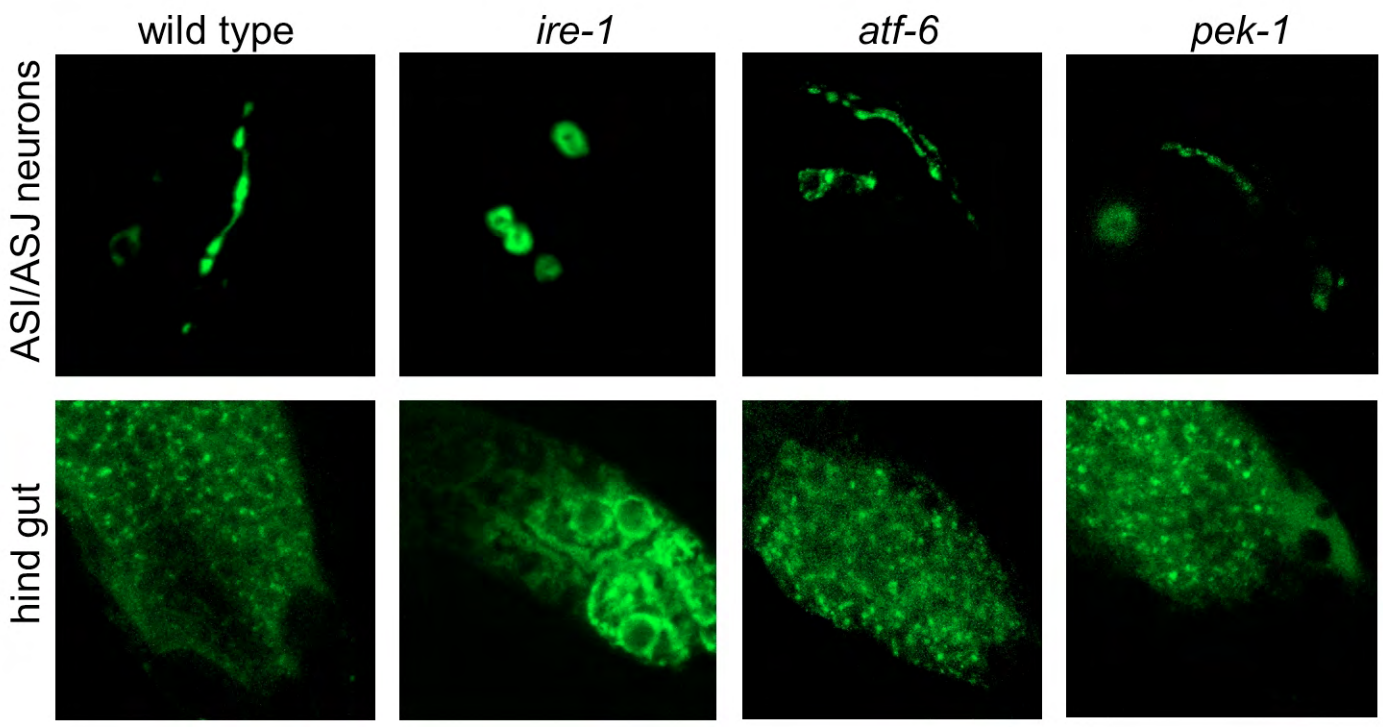

Fig. S2. *ire-1* deficiency alters DAF-28::GFP pattern within producing cells. Confocal fluorescence micrographs (630×) of ASI/ASJ neurons and hind gut in day-3 wild-type animals and in *ire-1, atf-6* and *pek-1* mutants.

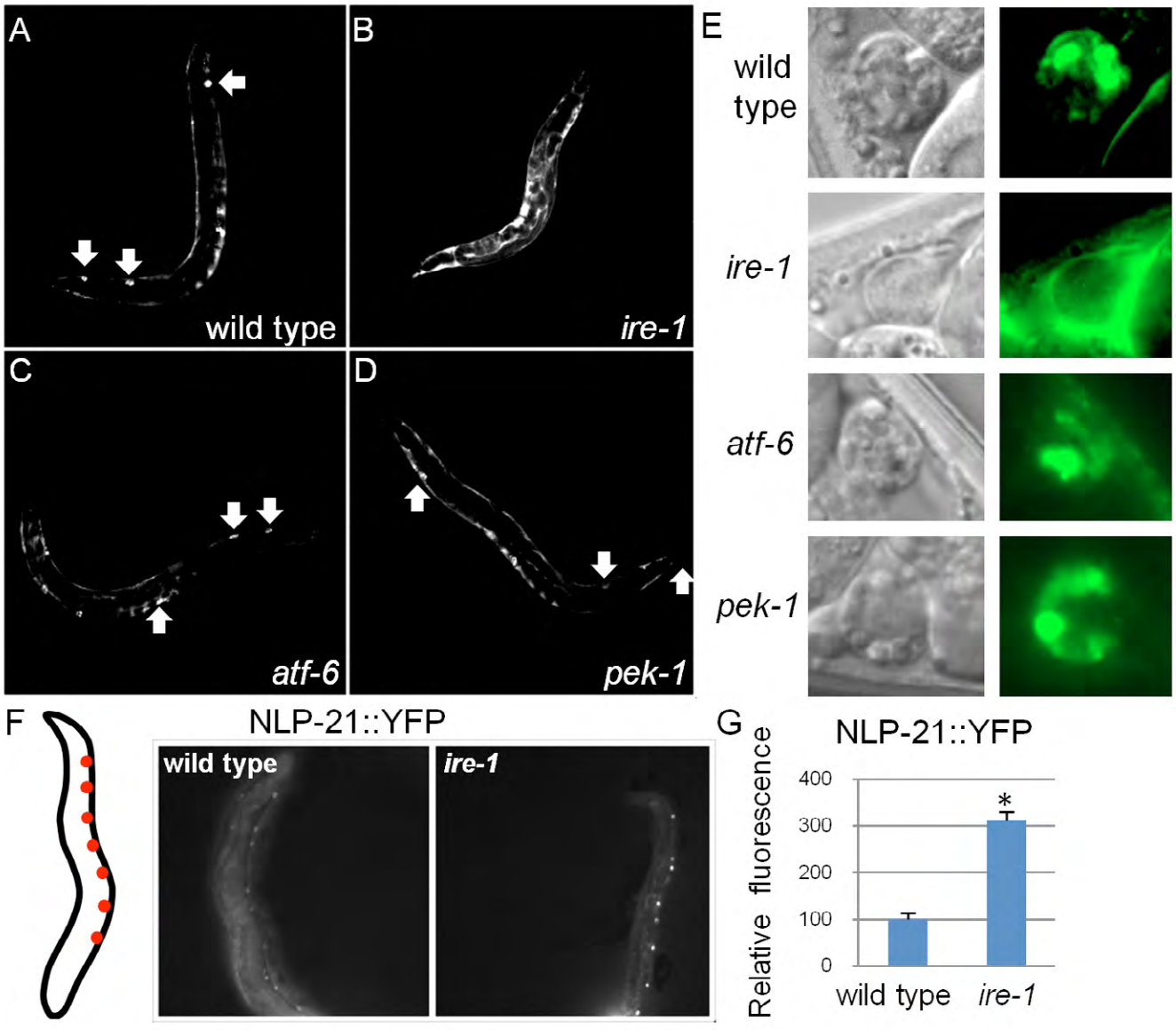

Fig. S3. *ire-1* deficiency alters *Pmyo-3*::ssGFP and *Punc-129*::NLP-21::YFP expression patterns. (A-D) Representative fluorescence micrographs (100×) of day-1 adults harboring an integrated *Pmyo-3*::ssGFP transgene in a wild-type, *ire-1(ok799), atf-6(ok551)* or *pek-1(ok275)* background. Wide arrows point to GFP-labeled coelomocytes. Note that in *ire-1* mutants no GFP-labeled coelomocytes were detected. Instead accumulation of GFP within the body cavity was detected. (E) Representative Nomarski and fluorescence micrographs (630×) of coelomocytes in day-1 adults harboring an integrated *Pmyo-3*::ssGFP transgene in the indicated genotypes. GFP was detected surrounding the coelomocytes rather than within the coelomocyte cells of *ire-1* mutants. (F) Representative fluorescence micrographs (100×) of day-1 adults expressing the *nlp-21::yfp* transgene using the ventral-cord *Punc-129* promoter. Scheme of predicted *unc-129* expressing cells (red) is shown to the left. (G) Bar graph of mean relative fluorescence in the ventral cord neurons of wild type and *ire-1* mutants. Fluorescence was measured in at least 20 animals per genotype. Similar results were obtained in three independent experiments. Asterisk marks Student's *t*-test value of $P<0.0001$.

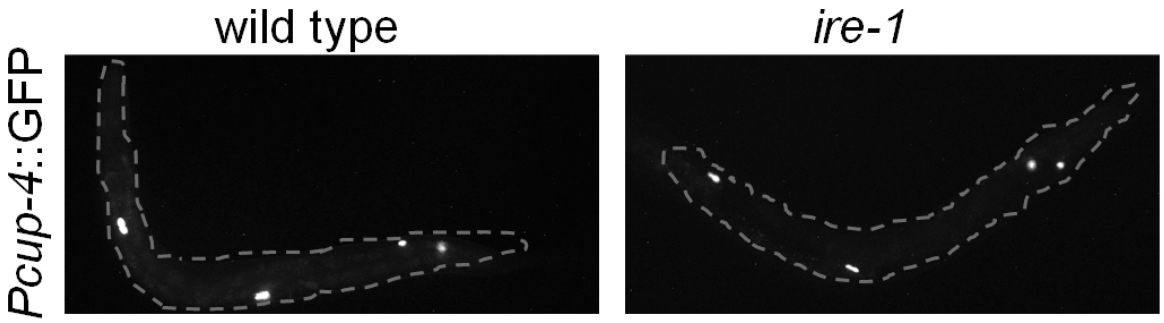

Fig. S4. Coelomocytes do exist in *ire-1* mutants. Representative fluorescence micrographs (100×) of day-1 adults harboring an integrated transgene expressing GFP under the coelomocyte-specific *cup-4* promoter.

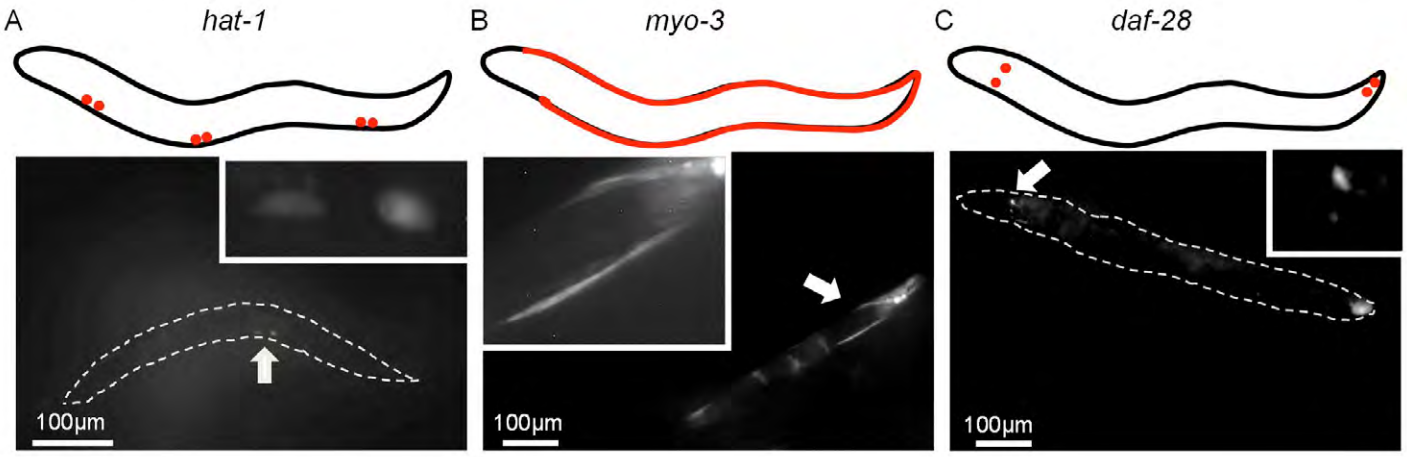

Fig. S5. Tissue-specific rescue of *ire-1* activity. Representative fluorescence micrographs of *Phsp-4::gfp* in *ire-1* mutants expressing *ire-1* under *hat-1*, *myo-3* and *daf-28* tissue-specific promoters. (A) Scheme and representative fluorescence micrograph (200×) of young animals expressing *ire-1* driven by the *hat-1* promoter. We note that *Phsp-4::gfp* induction was detected only in coelomocyte cells. No induction was detected outside of the coelomocytes in more than 50 animals examined. Induction was always detected only in 1-2 coelomocyte cells per animal. (B) Scheme and representative fluorescence micrograph (100×) of young animals expressing *ire-1* driven by the *myo-3* promoter. We note that *Phsp-4::gfp* induction was detected only in muscle cells. More than 50 animals were examined. (C) Scheme and fluorescence micrograph (100×) of young animals expressing *ire-1* driven by the *daf-28* promoter. In all animals examined, *Phsp-4*::GFP expression was detected in a few head neurons (most likely the ASI/ASJ neurons). In some animals, *Phsp-4*::GFP expression was also detected in the hind gut. Note that due to the long exposure times, some autofluorescence, clearly distinguishable from the GFP signal, was detected as well. Wide white arrows point at *Phsp-4::gfp*-expressing cells whose magnified images are presented in the corresponding insets.

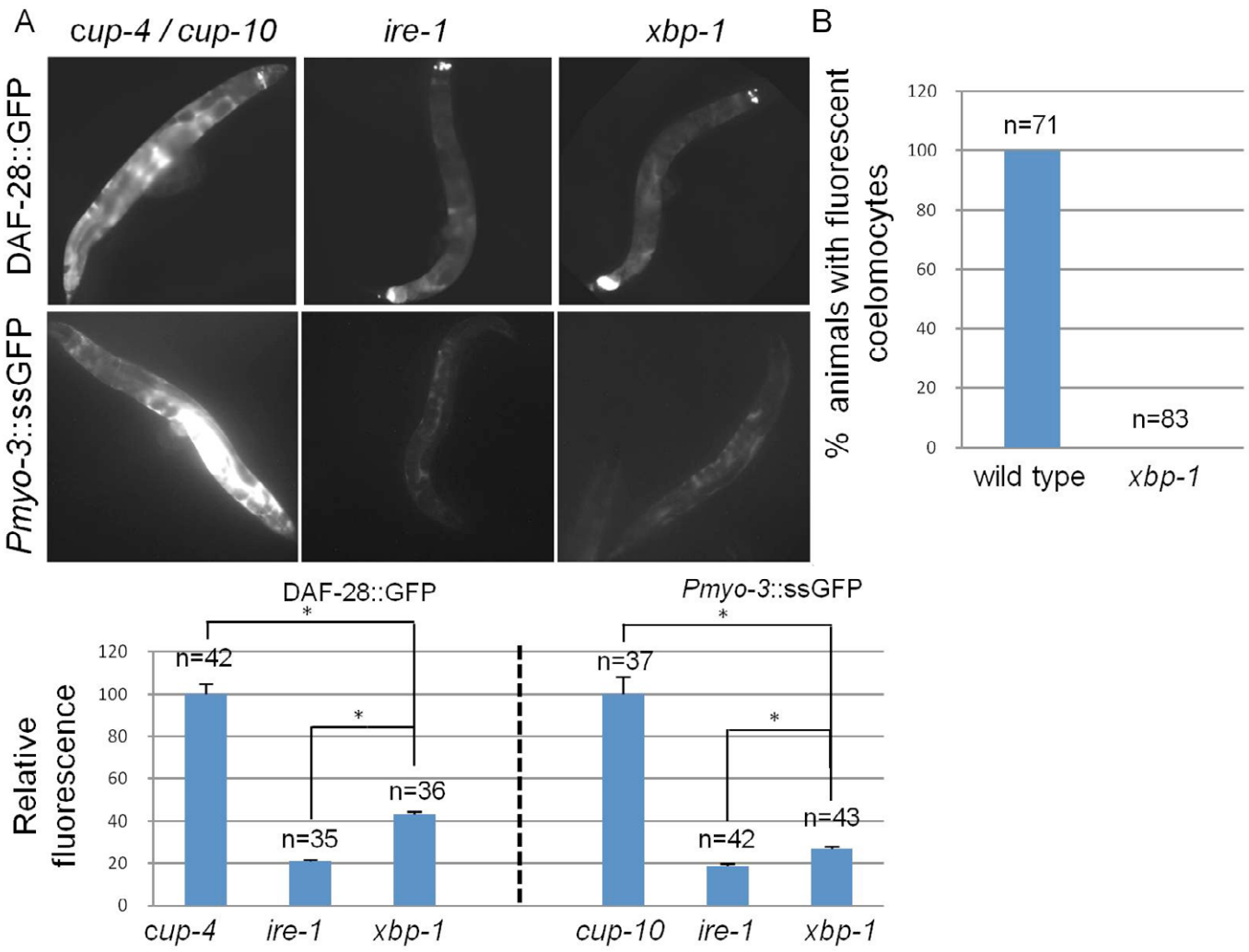

Fig. S6. *xbp-1* deficiency reduces accumulation of secreted proteins in the body cavity of coelomocyte-defective animals. (A) Representative fluorescence micrographs (100×) of day-3 adults harboring an integrated DAF-28::GFP transgene (upper panel), or day-1 adults harboring a *Pmyo-3*::ssGFP transgene (lower panel). Bar graphs of the mean whole body fluorescence in the corresponding strains is presented. Coelomocyte-defective *cup-4(ok837)* and *cup-10(ar479)* mutants accumulate fluorescent proteins in their body cavities. Coelomocyte-defective *ire-1(ok799*) and *xbp-1(tm2457)* mutants accumulate significantly less GFP in their body cavities. "n" indicates number of animals analyzed. Similar results were obtained in three independent experiments. Asterisks mark Student's *t*-test values of $P<0.0001$ of *xbp-1* mutants compared to wild-type animals and compared to *ire-1* mutants. (B) Percentage of wild-type animals and *xbp-1* mutants in which fluorescent coelomocytes were detected. "n" indicates number of animals analyzed.

Table S1. Worm strains

N_2

CF2473: *ire-1(ok799) II*;

CF3208: *xbp-1*(*tm2475*) *III*;

CF2921: *pek-1(ok275) X;*

CF2988: *atf-6(ok551) X*;

GR1455: *mgIs40[Pdaf-28::gfp];*

CF3222: *ire-1(ok799) II*; *mgIs40[Pdaf-28::gfp]*;

VB1605: *svIs69[Pdaf-28::DAF-28::GFP];*

SHK11: *ire-1(ok799) II*; *svIs69[Pdaf-28::daf-28::gfp] ;*

xbp-1(tm2457) III; svIs69[Pdaf-28::daf-28::gfp] ;

SHK38: *cup-4(ok837) III; svIs69[Pdaf-28::daf-28::gfp] ;*

SHK15: *ire-1(ok799) II*; *svIs69[Pdaf-28::daf-28::gfp] ;biuEx4[Pdaf-28::ire-1; pRF4(rol-6(su1006))];*

SHK17: *ire-1(ok799) II*; *svIs69[Pdaf-28::daf-28::gfp] ;biuEx3[Phat-1::ire-1; pRF4(rol-6(su1006))];*

SHK18: *ire-1(ok799) II*; *svIs69[Pdaf-28::daf-28::gfp] ;*

SHK47: *pek-1(ok275) X*; *svIs69[Pdaf-28::daf-28::gfp] ;*

SHK48: *atf-6(ok551) X*; *svIs69[Pdaf-28::daf-28::gfp] ;*

SHK49*: biuEx7[Pdaf-28::ssRFP::KDEL; pRF4(rol-6(su1006))];*

SHK50: *ire-1(ok799) II; biuEx7[Pdaf-28::ssRFP::KDEL; pRF4(rol-6(su1006))];*

GS1912:arIs37[Pmyo-3::ssGFP] I; dpy-20(e1282) IV; mtm-9(ar479) V;

SHK12: *arIs37[Pmyo-3::ssGFP] I; ire-1(ok799) II*;

arIs37[Pmyo-3::ssGFP] I; xbp-1(tm2457) III;

GS2495: *arIs37[Pmyo-3::ssGFP] I; cup-10*(ar479) *V*;

SHK13: *arIs37[Pmyo-3::ssGFP] I*; *ire-1(ok799) II*; *biuEx3[Phat-1::ire-1; pRF4(rol-6(su1006)] ;*

SHK14: *arIs37[Pmyo-3::ssGFP] I*; *ire-1(ok799) II*; *biuEx5[Pmyo-3::ire-1; pRF4(rol-6(su1006))] ;*

KP3947*: nuIs183[Punc-129::nlp-21::Venus; Pmyo-2::GFP] III;*

SHK21: *ire-1(ok799*) II; *nuIs183[Punc-129::nlp-21::Venus; Pmyo-2::GFP] III ;*

CL4176: *smg-1(cc546) I*; *dvIs27[pAF29(Pmyo-3/A-Beta 1-42/let UTR) + pRF4(rol-6(su1006))];*

SHK39: *smg-1(cc546) I*; *xbp-1(tm2457) III*; *dvIs27[pAF29(Pmyo-3/A-Beta 1-42/let UTR) + pRF4(rol-6(su1006))];*

SHK51: *smg-1(cc546) I*; *ire-1(ok799) II*; *dvIs27[pAF29(Pmyo-3/A-Beta 1-42/let UTR) + pRF4(rol-6(su1006))];*

SHK34: *arIs37[Pmyo-3::ssGFP] I; pek-1 (ok275) X*;

SHK33: *arIs37[Pmyo-3::ssGFP] I; atf-6 (ok5551) X;*

SHK29: *ire-1(ok799) II*; *cdIS42[Pcup-4::GFP; unc-119+];*

NP748: *unc119(ed3) III; cdIS42[Pcup-4::GFP; unc-119+];*

ire-1(ok799) II; *zcIs4[hsp-4::GFP]* V; *biuEx3[Phat-1::ire-1; pRF4(rol-6(su1006))];*

ire-1(ok799) II; *zcIs4[hsp-4::GFP]* V;*biuEx5[Pmyo-3::ire-1; pRF4(rol-6(su1006))] ;*

ire-1(ok799) II; *zcIs4[hsp-4::GFP]* V;*biuEx4[Pdaf-28::ire-1; pRF4(rol-6(su1006))] ;*

ire-1(ok799) is a null mutation in which three exons containing the kinase and endonuclease domains are deleted.

xbp-1(zc12) is a putative null mutation, a nonsense mutation that changes Q34 to an ochre stop, terminating it before its functional domains. Similarly to *xbp-1(tm2475)* null mutants, animals carrying zc12 are sensitive to ER stress and unable to induce transcription through the *hsp-4* promoter in response to ER stress.

atf-6(ok551) is a putative null mutation deleting 1,900 bp of genomic sequence, resulting in a protein missing the leucine zipper portion of the bZIP domain, the transmembrane domain, and the ER luminal domain.

pek-1(ok275) is a putative null mutation in which more than five exons are missing, resulting in the loss of a critical transmembrane domain.